Supporting Information

Tagliazucchi et al. 10.1073/pnas.0913340107

SI Text

Theoretical Approach. The system that we describe consists of N_p polyacids end-grafted to a surface of total area A. The probability of finding chain $j (j = 1, N_p)$ in conformation α is given by $P_P(j, \alpha)$. The polymer chain consists of n monomer units, each one bearing an acid group that can be either protonated (HAc) or deprotonated (Ac). The theory is derived by expressing the free energy of the system as a functional of the polymer probabilities, the density distribution of all the free molecular species in solution, and the interaction fields. The free species include: water (w), cations (C), and anions (A) from the solution dissociated added salt, protons (H^+), and hydroxyl ions (OH^-). The total free energy is given by

$$F = -TS_{\text{mix}} - TS_{\text{conf}} + E_{\text{vdw}} + E_{\text{rep}} + E_{\text{elec}} + F_{\text{chem}},$$

where T is the absolute temperature and in terms of the density of the different species, the probability of chain conformations and the interactions fields is

$$\begin{aligned}
\beta F = & \int \rho_w(\mathbf{r})[\ln(\rho_w(\mathbf{r})\nu_w) - 1]d\mathbf{r} + \int \rho_A(\mathbf{r})[\ln(\rho_A(\mathbf{r})\nu_w) - 1]d\mathbf{r} \\
& + \int \rho_C(\mathbf{r})[\ln(\rho_C(\mathbf{r})\nu_w) - 1]d\mathbf{r} \\
& + \int \rho_{H^+}(\mathbf{r})[\ln(\rho_{H^+}(\mathbf{r})\nu_w) - 1 + \mu^0_{H^+}]d\mathbf{r} \\
& + \int \rho_{OH^-}(\mathbf{r})[\ln(\rho_{OH^-}(\mathbf{r})\nu_w) - 1 + \mu^0_{OH^-}]d\mathbf{r} \\
& + \sum_j^{N_P} \sum_\alpha P_P(j,\alpha) \ln P_P(j,\alpha) \\
& + \iint \frac{\beta\chi g(|\mathbf{r}-\mathbf{r}'|)}{2} \langle\phi_P(\mathbf{r})\rangle\langle\phi_P(\mathbf{r}')\rangle d\mathbf{r}d\mathbf{r}' \\
& + \int \left[\langle\rho_Q(\mathbf{r})\rangle\beta\psi(\mathbf{r}) - \frac{1}{2}\varepsilon\beta(\nabla\psi(\mathbf{r}))^2\right]d\mathbf{r} \\
& + \int \langle n_P(\mathbf{r})\rangle[f_c(\mathbf{r})[\ln(f_c(\mathbf{r})) + \beta\mu^0_{Ac^-}] \\
& + (1-f_c(\mathbf{r}))[\ln(1-f_c(\mathbf{r})) + \beta\mu^0_{HAc}]]d\mathbf{r} \qquad \textbf{[S1]}
\end{aligned}$$

where $\beta = 1/k\text{T}$ and $\mathbf{r}$ is the position vector and the integrals run over the whole space. The first five terms in Eq. **1** are the translational (mixing) entropies of the mobile species. $\rho_i(\mathbf{r})$ is the number density of species i ($i = w, C, A, H^+$ and OH^-, respectively) at position $\mathbf{r}$ and $\mu^0_{H^+}$ and $\mu^0_{OH^-}$ are the standard chemical potentials of protons and hydroxyl ions, resp. The sixth term is the conformational entropy of the polyelectrolyte chains. The next term is the van der Waals (vdW) effective attractive energy between polymer beads (1) that represents the hydrophobicity of the backbone. χ is the strength of the attractive interactions, i.e., a measure of the hydrophobicity, and $g(\mathbf{r}-\mathbf{r}')$ is a distance dependent van der Waals attractive term (see below). $\langle\phi_P(\mathbf{r})\rangle$ is the volume fraction of the polymer at $\mathbf{r}$. The critical parameter χ_c is that required to induce microphase segregation in a neutral polymer layer in the limit of vanishing surface coverage and it is close to the Θ conditions for the polymer backbone (2). Thus, $\chi_c/\chi > 1$ and $\chi_c/\chi < 1$ correspond to less and more hydrophobic backbones (good and poor solvent conditions in polymer literature), resp.

The eight term in Eq. **1** is the electrostatic contribution to the free energy, where $\Psi(\mathbf{r})$ is the local electrostatic potential, ϵ is the dielectric constant, and $\langle\rho_Q(\mathbf{r})\rangle$ is the average charge density at $\mathbf{r}$, given by $\langle\rho_Q(\mathbf{r})\rangle = \sum_i \rho_i(\mathbf{r})q_i + \langle n_P(\mathbf{r})\rangle f_c(\mathbf{r})q_P$, where the sum runs over all charged mobile species and $\langle n_P(\mathbf{r})\rangle$ is the average number density of polymer segments at $\mathbf{r}$, q_i is the charge of species i in units of the elemental charge, and $f_c(\mathbf{r})$ is the fraction of charged acid groups at $\mathbf{r}$. Note that the fraction of charged acid groups depends on the position and therefore segments located in different regions of the system can present different protonation states. The last contribution to the free energy functional is the mixing entropy between charged and uncharged groups, with $\mu^0_{Ac^-}$ and μ^0_{HAc} being their respective standard chemical potentials. The standard chemical potentials are related to the acid-base equilibrium constant of an isolated group in the bulk by $K_a = C\exp[-\beta\mu^0_{H^+} - \beta\mu^0_{Ac^-} + \beta\mu^0_{HAc}]$ (3), where C is a constant. Note that the excluded volume repulsive interactions between segments (the term E_{rep}) is not explicitly included in Eq. **1**. As we explain below, this contribution is considered in the chain generation process for intramolecular repulsions (only self-avoiding conformations are included) and through packing constraints for the intermolecular repulsions (3, 4), see Eq. **2** below.

Under the approximation of lateral homogeneity, the free energy of the 3D theory (Eq. **1**) can be simplified to the free energy of the 1D molecular theory (2, 3), allowing straightforward comparison between them. Note that the 1D molecular theory enables to find the onset of instability of the homogeneous brush but cannot predict the morphologies of the aggregates. Namely, it provides with the yes or no answer to the question of stability.

The unknowns in Eq. **1** are the position dependent densities of mobile species, the probability distribution functions for each chain $P_P(j, \alpha)$, the electrostatic potential, and the fraction of charged groups. They are found by a functional minimization of the free energy subject to the packing constraints. The input necessary for the theory includes a large representative set of unbiased polymer conformations, the positions of the grafting points, χ_c/χ, the bulk pK_a for the isolated acid groups, and the experimentally controlled variables: i.e., bulk pH and salt concentration. The output includes all the average structural information as well as the values of all the thermodynamic quantities.

Minimization of the Free Energy Functional. The minimization of Eq. **1** is subject to two constraints. The packing or incompressibility constraint takes into account the intermolecular repulsions for each $\mathbf{r}$:

$$\begin{aligned}
& \rho_A(\mathbf{r})\nu_A + \rho_C(\mathbf{r})\nu_C + \rho_{H^+}(\mathbf{r})\nu_{H^+} \\
& \quad + \rho_{OH^-}(\mathbf{r})\nu_{OH^-} + \rho_w(\mathbf{r})\nu_w + \langle\phi_P(\mathbf{r})\rangle = 1, \qquad \textbf{[S2]}
\end{aligned}$$

where the total polymer volume fraction, $\langle\phi_P(\mathbf{r})\rangle$, is given by

$$\langle\phi_P(\mathbf{r})\rangle = \sum_j^{N_P} \sum_\alpha P_P(\alpha, j) n_P(\mathbf{r}, \alpha, j)\nu_P \qquad \textbf{[S3]}$$

with $n_P(\mathbf{r}, \alpha, j)$ the number of segments that the jth chain in the system has at $\mathbf{r}$ when it is in conformation α.

The other requirement is the global electroneutrality, given by:

$$\int \langle\rho_Q(\mathbf{r})\rangle d\mathbf{r} = 0. \qquad \textbf{[S4]}$$

Here, $\langle \rho_Q(\mathbf{r}) \rangle$ is the average density of charges at $\mathbf{r}$:

$$\langle \rho_Q(\mathbf{r}) \rangle = \langle n_P(\mathbf{r}) \rangle f_c(\mathbf{r}) q_{Ac^-} + \rho_A(\mathbf{r}) q_A + \rho_C(\mathbf{r}) q_C + \rho_{H^+}(\mathbf{r}) q_{H^+} + \rho_{OH^-}(\mathbf{r}) q_{OH^-} \quad [S5]$$

with $\langle n_P(\mathbf{r}) \rangle$ being the average number of polymer segments at $\mathbf{r}$, given by

$$\langle n_P(\mathbf{r}) \rangle = \sum_j^{N_P} \sum_\alpha P_P(\alpha, j) n_P(\mathbf{r}, \alpha, j). \quad [S6]$$

The packing (**2**) and electroneutrality (**4**) constraints are fulfilled by introducing the Lagrange multipliers $\pi(\mathbf{r})$ and λ, resp. The surface is in equilibrium with the bulk solution that provides a bath for protons, hydroxyl ions, cations, and anions. Therefore, to fulfill the thermodynamic requirement of constant chemical potential for all the free species everywhere in the system, i.e., at all $\mathbf{r}$, we consider a Legendre transform of the free energy, F. The presence of two constrains reduces the number of independent thermodynamic variables and we do not need to consider the chemical potentials of protons, hydroxyls ions and solvent molecules (3). We write a semi-grand canonical potential, including the constraints and chemical potentials of anions and cations:

$$\beta W = \beta F + \int \beta \pi(\mathbf{r}) \left[\sum_i \rho_i(\mathbf{r}) \nu_i + \langle \phi_P(\mathbf{r}) \rangle - 1 \right] d\mathbf{r} + \lambda \int \langle \rho_Q(\mathbf{r}) \rangle d\mathbf{r} - \beta \mu_C \int \rho_C(\mathbf{r}) d\mathbf{r} - \beta \mu_A \int \rho_A(\mathbf{r}) d\mathbf{r} \quad [S7]$$

and find its extremum with respect to $\rho_i(\mathbf{r})$, $f_c(\mathbf{r})$, $\Psi(\mathbf{r})$, and $P_p(\alpha, j)$. It can be proven that λ, enforcing the electroneutrality condition, is a constant term added to the electrostatic potential and therefore it can included in the choice of boundary conditions (4). $\pi(\mathbf{r})$ is a position-dependant osmotic pressure (3, 5).

The variation, with respect to $P_p(\alpha, j)$, leads to the probability distribution function for the polymer chains:

$$P_P(\alpha, j) = \frac{1}{\xi(j)} \exp\left[- \int n_P(\mathbf{r}, \alpha, j) [\ln(f_c(\mathbf{r})) + q_{Ac^-} \beta \psi(\mathbf{r}) + \beta \mu^0_{Ac^-}] d\mathbf{r} - \int \nu_P(\mathbf{r}, \alpha, j) [\beta \pi(\mathbf{r}) + \int \beta \chi g(|\mathbf{r} - \mathbf{r}'|) \langle \phi_P(\mathbf{r}') \rangle d\mathbf{r}'] d\mathbf{r} \right]. \quad [S8]$$

In Eq. **8**, $\xi(j)$ is the partition function of molecule j (normalization constant that assures $\Sigma_\alpha P_p(\alpha, j) = 1$).

Minimization of eq. (**7**) with respect to $\rho_i(\mathbf{r})$ yields the local densities of the anion, cation, proton, hydroxyl, and solvent:

$$\rho_A(\mathbf{r}) \nu_w = \exp[-\nu_A \beta \pi(\mathbf{r}) + \beta \mu_A - q_A \beta \psi(\mathbf{r})], \quad [S9]$$

$$\rho_C(\mathbf{r}) \nu_w = \exp[-\nu_C \beta \pi(\mathbf{r}) + \beta \mu_C - q_C \beta \psi(\mathbf{r})], \quad [S10]$$

$$\rho_{H^+}(\mathbf{r}) \nu_w = \exp[-\nu_{H^+} \beta \pi(\mathbf{r}) - \beta \mu^0_{H^+} - q_{H^+} \beta \psi(\mathbf{r})], \quad [S11]$$

$$\rho_{OH^-}(\mathbf{r}) \nu_w = \exp[-\nu_{OH^-} \beta \pi(\mathbf{r}) - \beta \mu^0_{OH^-} - q_{OH^-} \beta \psi(\mathbf{r})], \quad [S12]$$

$$\rho_w(\mathbf{r}) \nu_w = \exp(-\nu_w \beta \pi(\mathbf{r})). \quad [S13]$$

By relating the chemical potentials of these species with the bulk densities, we can rewrite Eqs. **9–13** in a more practical way:

$$\rho_A(\mathbf{r}) \nu_w = \rho^{bulk}_A \nu_w \exp(-\nu_A \beta [\pi(\mathbf{r}) - \pi^{bulk}] - q_A \beta [\psi(\mathbf{r}) - \psi^{bulk}]), \quad [S14]$$

$$\rho_C(\mathbf{r}) \nu_w = \rho^{bulk}_C \nu_w \exp(-\nu_C \beta [\pi(\mathbf{r}) - \pi^{bulk}] - q_C \beta [\psi(\mathbf{r}) - \psi^{bulk}]), \quad [S15]$$

$$\rho_{H^+}(\mathbf{r}) \nu_w = \rho^{bulk}_{H^+} \nu_w \exp(-\nu_{H^+} \beta [\pi(\mathbf{r}) - \pi^{bulk}] - q_{H^+} \beta [\psi(\mathbf{r}) - \psi^{bulk}]), \quad [S16]$$

$$\rho_{OH^-}(\mathbf{r}) \nu_w = \rho^{bulk}_{OH^-} \nu_w \exp(-\nu_{OH^-} \beta [\pi(\mathbf{r}) - \pi^{bulk}] - q_{OH^-} \beta [\psi(\mathbf{r}) - \psi^{bulk}]), \quad [S17]$$

$$\rho_w(\mathbf{r}) \nu_w = \rho^{bulk}_w \nu_w \exp(-\nu_w \beta [\pi(\mathbf{r}) - \pi^{bulk}]). \quad [S18]$$

The variation of the potential W, Eq. **7**, with respect to $f_c(\mathbf{r})$ yields:

$$\ln\left(\frac{f_c(\mathbf{r})}{1 - f_c(\mathbf{r})} \right) = -\beta \mu^0_{H^+} - \beta \mu^0_{Ac^-} + \beta \mu^0_{HAc} - \nu_{H^+} \beta \pi(\mathbf{r}) - \ln(\rho_{H^+}(\mathbf{r}) \nu_w). \quad [S19]$$

This equation can be rewritten to resemble the more familiar acid-base equilibrium equation:

$$K^0_a = \exp[-\beta \Delta G^0_c] = \rho_{H^+}(\mathbf{r}) \nu_w \frac{f_c(\mathbf{r})}{1 - f_c(\mathbf{r})} \exp(\nu_{H^+} \beta \pi(\mathbf{r})). \quad [S20]$$

Here, $\Delta G^0_c = \mu^0_{H^+} + \mu^0_{Ac^-} - \mu^0_{HAc}$ is the standard reaction free energy and K^0_a is the thermodynamic equilibrium constant for deprotonation reaction. The latter can be multiplied by the constant factor ρ^{bulk}_w / N_A (with N_A equal to Avogadro's number) to obtain the commonly used equilibrium constants based on molar bulk concentrations (3).

The extremum of W, with respect to $\Psi(\mathbf{r})$, gives rise to a generalized Poisson–Boltzmann equation for the electrostatic potential:

$$\varepsilon \nabla^2 \psi(\mathbf{r}) = -\langle \rho_Q(\mathbf{r}) \rangle. \quad [S21]$$

The boundary conditions for Eq. **21** are:

$$\lim_{z \to \infty} \psi(\mathbf{r}) = 0 \quad [S22]$$

and, for an uncharged surface,

$$\frac{\partial \psi}{\partial z}(\mathbf{r}) \Big|_{z=0} = 0. \quad [S23]$$

Implementation of Periodic Boundary Conditions (PBC). The 3D molecular theory was formulated above for a system that is semi-infinite in the direction normal to the surface (z) and infinite in the planes parallel to it. To solve the theory, we consider periodic boundary conditions in the planes parallel to the surface. It is natural to choose a hexagonal arrangement of grafting points (Fig. S1). We have also carried out calculations with a square arrangement of grafting points and found no discernible differences in the morphologies of the domains. Here, we explicitly describe the calculations with hexagonal arrangement because they are the ones presented in the manuscript.

The implementation of the hexagonal distribution of grafting points with PBC in the planes parallel to the surface requires the choice of a coordinate system that is different from the orthogonal x,y,z Cartesian coordinates. In the ν,u,z coordinate system, the ν and u axes are at 60° angle (Fig. S1). It is obtained by the following transformations from the Cartesian coordinates:

$$\nu = \frac{\cos(\pi/12)x - \sin(\pi/12)y}{\sqrt{\cos^2(\pi/12) - \sin^2(\pi/12)}}, \quad \textbf{[S24]}$$

$$u = \frac{-\sin(\pi/12)x + \cos(\pi/12)y}{\sqrt{\cos^2(\pi/12) - \sin^2(\pi/12)}}, \quad \textbf{[S25]}$$

$$z = z. \quad \textbf{[S26]}$$

The Laplacian operator in the Poisson equation, Eq. **21** in hexagonal coordinates is:

$$\begin{aligned}\nabla^2 &= \frac{\partial^2}{\partial x^2} + \frac{\partial^2}{\partial y^2} + \frac{\partial^2}{\partial z^2} \\ &= \left(\frac{1}{\cos^2(\pi/12) - \sin^2(\pi/12)}\right)\left[\frac{\partial^2}{\partial \nu^2} + \frac{\partial^2}{\partial u^2}\right. \\ &\quad \left. - 4\sin(\pi/12)\cos(\pi/12)\frac{\partial^2}{\partial u \partial \nu}\right] + \frac{\partial^2}{\partial z^2}. \quad \textbf{[S27]}\end{aligned}$$

The periodic boundary conditions for a function of **r** in an hexagonal periodic cell and using hexagonal coordinates are:

$$f(\nu + N_\nu L_\nu, u + N_u L_u, z) = f(\nu, u, z), \quad \textbf{[S28]}$$

where L_ν and L_u are the dimensions of the periodic box in the ν and u directions and N_ν and N_u are integers. The molecular theory is then discretized and solved in the hexagonal coordinates. The functions for the density of mobile species, polymer volume fraction, electrostatic potential, and fraction of charged groups are then casted back to Cartesian coordinates for visualization. The coordinates of point (ν,u,z) in the hexagonal system are converted to a point (x,y,z) in the Cartesian system by using the following relationships:

$$x = \frac{\cos(\pi/12)\nu + \sin(\pi/12)u}{\sqrt{\cos^2(\pi/12) - \sin^2(\pi/12)}}, \quad \textbf{[S29]}$$

$$y = \frac{\sin(\pi/12)\nu + \cos(\pi/12)u}{\sqrt{\cos^2(\pi/12) - \sin^2(\pi/12)}}, \quad \textbf{[S30]}$$

$$z = z. \quad \textbf{[S31]}$$

Numerical Solution. To obtain numerical results from the molecular theory, we must solve the nonlinear integro–differential equation system that results from substituting expressions (**8**, **14**–(**19**) into the packing constrain, Eq. **2** and the generalized Poisson–Boltzmann equation, Eq. **21**. To do that, we discretize the ν, u and z coordinates into cells of dimesions $\delta \times \delta \times \delta$. From preliminary calculations we have chosen a discretization step of $\delta = 0.5$ nm. The numbers of discretization cells along the ν and u axis, M_ν and M_u, are L_ν/δ and L_u/δ. The size of the periodic box was chosen to be larger than the morphologies under study, but to be small enough to allow systematic calculations. In this work, we considered 64 chains in our periodical cell and, therefore, L_ν and L_u range from 40 to 72 depending on the grafting density. We also performed some calculations with a periodic cell of 144 chains that yielded very similar results. The z-direction is in principle semi-infinite but, in practice, we consider a distance from the surface long enough to guarantee the asymptotic convergence of electrostatic potential and the concentrations of the free species to their bulk value. Typical values of the number of cells along the z-direction (M_z) range from 40 to 80. The total number of cells in the system is, thus, of the order of 10^5. The equations obtained by minimizing the free energy are discretized by replacing integrals by sums and derivatives by finite differences. Finally, we arrive to a set of the order of 10^5 equations (twice the number of cells in the system) that is solved by using Jacobian–Free Newton method and a parallel implementation.

To solve the discretized equations, we should start with an initial guess. While we have observed spontaneous symmetry breaking even with totally symmetric initial guesses, we found more convenient to use asymmetric initial guesses. For a given condition, different initial guesses yield in general the same morphology but with different specific details that correspond to different local minima of the free energy. We tried different initial guesses for each condition (in particular for those in the boundaries between morphologies) and chose the equilibrium state to be the one with the lowest free energy.

The discretized packing constraint, Eq. **2** and the generalized Poisson–Boltzmann equation, Eq. **21**, are given by:

$$\begin{aligned}&\rho_A(k,l,m)\nu_A + \rho_C(k,l,m)\nu_C + \rho_{H^+}(k,l,m)\nu_{H^+} \\ &\quad + \rho_{OH^-}(k,l,m)\nu_{OH^-} + \rho_w(k,l,m)\nu_w + \langle\phi_P(k,l,m)\rangle = 1 \quad \textbf{[S32]}\end{aligned}$$

and

$$\begin{aligned}&\left(\frac{1}{\cos^2(\pi/12) - \sin^2(\pi/12)}\right)[\psi(k+1,l,m) - 2\psi(k,l,m) \\ &\quad + \psi(k-1,l,m) \\ &\quad + \psi(k,l+1,m) - 2\psi(k,l,m) + \psi(k,l-1,m) \\ &\quad - \sin(\pi/12)\cos(\pi/12). \\ &\quad \times \{\psi(k+1,l+1,m) - \psi(k+1,l-1,m) - \psi(k-1,l+1,m) \\ &\quad + \psi(k-1,l-1,m)\}] \\ &\quad + \{\psi(k,l,m+1) - 2\psi(k,l,m) + \psi(k,l,m-1) \\ &\quad = -\langle\rho_Q(k,l,m)\rangle\delta^2/\varepsilon \quad \textbf{[S33]}\end{aligned}$$

Note that the continuous indexed ν, u, and z have been replaced by the integers k, l, and m. These three indexes define cells in the periodic box that can take values between one and M_ν, M_u, or M_z, resp. When a value outside the cell is needed in the ν, u plane (i.e., boundary cells in Eq. **33**), a discretized form of the PBC in Eq. **28** is used:

$$f(k + N_\nu M_\nu, l + N_u M_u, m) = f(k,l,m). \quad \textbf{[S34]}$$

The terms required to solve the system of coupled Eqs. **32** and **33** are the discretized forms of Eqs. **8** and **14**–**19**.

The densities of mobile species are:

$$\begin{aligned}\rho_A(k,l,m)\nu_w = \rho_A^{bulk}\nu_w \exp(&-\nu_A\beta[\pi(k,l,m) - \pi^{bulk}] \\ &- q_A\beta[\psi(k,l,m) - \psi^{bulk}]), \quad \textbf{[S35]}\end{aligned}$$

$$\begin{aligned}\rho_C(k,l,m)\nu_w = \rho_C^{bulk}\nu_w \exp(&-\nu_C\beta[\pi(k,l,m) - \pi^{bulk}] \\ &- q_C\beta[\psi(k,l,m) - \psi^{bulk}]), \quad \textbf{[S36]}\end{aligned}$$

$$\rho_{H^+}(k,l,m)\nu_w = \rho_{H^+}^{bulk}\nu_w \exp(-\nu_{H^+}\beta[\pi(k,l,m) - \pi^{bulk}] - q_{H^+}\beta[\psi(k,l,m) - \psi^{bulk}]), \quad \text{[S37]}$$

$$\rho_{OH^-}(k,l,m)\nu_w = \rho_{OH^-}^{bulk}\nu_w \exp(-\nu_{OH^-}\beta[\pi(k,l,m) - \pi^{bulk}] - q_{OH^-}\beta[\psi(k,l,m) - \psi^{bulk}]), \quad \text{[S38]}$$

$$\rho_w(k,l,m)\nu_w = \rho_w^{bulk}\nu_w \exp(-\nu_w\beta[\pi(k,l,m) - \pi^{bulk}]). \quad \text{[S39]}$$

The fraction of charged groups is given by

$$\ln\left(\frac{f_c(k,l,m)}{1-f_c(k,l,m)}\right) = -\beta\mu_{H^+}^0 - \beta\mu_{Ac^-}^0 + \beta\mu_{HAc}^0 - \nu_{H^+}\beta\pi(k,l,m) - \ln(\rho_{H^+}(k,l,m)\nu_w). \quad \text{[S40]}$$

Finally, the PDFs for the polymer are:

$$P_P(\alpha,j) = \frac{1}{\xi(j)}\exp\left\{-\sum_{k,l,m} n_P(k,l,m,\alpha,j)[\ln(f_c(k,l,m)) + q_{Ac^-}\beta\psi(k,l,m)] - \sum_{k,l,m}\nu_P(k,l,m,\alpha,j)\left[\beta\pi(k,l,m) + \sum_{k',l',m'}\beta\chi g(k-k',l-l',m-m')\langle\phi_P(k',l',m')\rangle\right]\right\}. \quad \text{[S41]}$$

In this equation, $\beta\mu_{A^-}^0$ is included in the normalization term. In the sums with indexes k', l', and m', the interaction with segments outside the periodic box should be considered by means of Eq. **34**.

The discretized function for $g(|\mathbf{r}-\mathbf{r}'|)$ is $g(k-k', l-l', m-m')$. This is obtained by integration of the vdW attractions in the cells of the hexagonal lattice by using a Monte Carlo procedure. More explicitly, we find the integrals

$$g(k-k',l-l',m-m') = \int_{\delta(k-k'-\frac{1}{2})}^{\delta(k-k'+\frac{1}{2})}\int_{\delta(l-l'-\frac{1}{2})}^{\delta(l-l'+\frac{1}{2})}\int_{\delta(m-m'-\frac{1}{2})}^{\delta(m-m'+\frac{1}{2})}\left(\frac{a}{|\mathbf{r}-\mathbf{r}'|}\right)^6 d\nu du dz \quad \text{[S42]}$$

constrained to $a < |\mathbf{r}| < 1.5\delta$, where a is the segment length.

Visualization and plotting of 3D functions have been performed with Paraview (www.paraview.org).

Molecular Model. We define here the molecular details of the species that are used in the calculations. The size and charge of the molecular species in the system are compiled in Table S1. The sums over all polymer conformations (e.g., in Eq. **6**) are treated approximately by considering a very large representative set of 5.10^5 conformations for each chain in the periodic box that are randomly generated in free space with the rotational-isomeric model (RIS) (6) where each segment bears an acid group and has a bond length of 3.5 Å. The model for the chain is one that we have used in earlier work and it provides a good representation of the chain conformations for a generic polyacid (3), for modeling a specific chemical polymer we can vary the bond length and segment volume and then obtain predictions in very good agreement with experimental observations (4, 7). We include in this set the 12 30° rotations around the z-axis for each randomly generated bond sequence to ensure that the set of polymer conformations does not introduce a bias toward some particular direction. We use the same set of conformations for each of the N_P polymers, with the only difference that each conformation is translated to have the first segment on each of the N_P grafting points. These points are placed in the centers of the discretization cells to assure the equivalency of all the chains in the system, thus, limiting the possible surface coverages that can be studied. The use of completely equivalent chain conformations in all the grafting points implies that the morphologies obtained are the result of spontaneous symmetry breaking in the free energy. Note, that the micelles are not all identical. This implies that this arrangement of the aggregates has a lower free energy than a system with identical micelles. The theory is capable of providing this detailed description because we explicitly include the inhomogeneities in all three dimensions.

Molecular Theory for Not-Regulating Polyacids. The formulation and implementation of the theory for non-regulating polyacids are similar to that for weak polyelectrolytes, but we drop the last term in Eq. **1** (entropy of mixing between protonated and unprotonated groups) and fix the fraction of charged groups for all **r** (all segments bear the same charge).

The phase diagram of the non-regulating polymers represented in a linear scale for the degree of dissociation f^{bulk} is given in Fig S2.

Simple analysis for the local pH within micellar aggregates. We propose, here, a simple analysis to explain the universal behavior observed in Fig. 4*D* for the dependence of the local pH inside the aggregates as a function of bulk conditions. Let us write the approximate expression for the Donnan potential inside the micelles for the case when the local concentration of negative charges ($\rho_{Qpol}^{micelle}$) is much higher than the ionic strength:

$$\Delta\phi_D = \frac{RT}{F}\ln\left(\frac{\rho_{QPol}^{micelle}}{C_{salt}}\right). \quad \text{[S43]}$$

This expression is only of approximate validity for the case of micellar aggregates in Fig. 4*D* because their size (5–10 nm) is comparable to the Debye length (0.96 nm for $C_{salt} = 0.1$ M, 6.8 nm for $C_{salt} = 0.002$ M) (8).

The local proton concentration inside the aggregates is approximately given by:

$$[H^+]^{micelle} = [H^+]^{bulk}.\exp\left(-\frac{F\Delta\phi_D}{RT}\right). \quad \text{[S44]}$$

Combining Eqs. **43** and **44** yields:

$$pH^{micelle} - pH^{bulk} = \log_{10}\left(\frac{C_{salt}}{\rho_{Qpol}^{micelle}}\right). \quad \text{[S45]}$$

We can now use Eq. **45** to consider both the regulating (weak) and the not-regulating grafted polyacid layers.

Regulating polyacid.
In this system, the fraction of charged segments inside the micelle is given by the local pH.

We can write:

$$\rho_{Qpol}^{micelle} = \rho_0^{micelle} f_c^{micelle} \quad \text{[S46]}$$

where $\rho_0^{micelle}$ is the concentration of polymer segments inside the aggregates (which is in the order of ~10 M) and $f_c^{micelle}$ is the fraction of these segments that are charged. We now write the expression for the acid-base chemical equilibrium inside the micelle:

$$\mathrm{pH}^{\mathrm{micelle}} = pK_a + \log_{10}\left(\frac{f_c^{\mathrm{micelle}}}{1 - f_c^{\mathrm{micelle}}}\right). \quad \textbf{[S47]}$$

In the conditions where micellar agreggates exists ($f_c^{\mathrm{micelle}} \ll 1$), we approximate Eq. **47** by:

$$\mathrm{pH}^{\mathrm{micelle}} = pK_a + \log_{10}(f_c^{\mathrm{micelle}}). \quad \textbf{[S48]}$$

We combine Eqs. **45**, **46**, and **48**:

$$\mathrm{pH}^{\mathrm{micelle}} - \mathrm{pH}^{\mathrm{bulk}} = \log_{10}\left(\frac{C_{\mathrm{salt}}}{\rho_0^{\mathrm{micelle}}}\right) - \mathrm{pH}^{\mathrm{micelle}} + pK_a \quad \textbf{[S49]}$$

and, after some rearrangements, obtain

$$\mathrm{pH}^{\mathrm{micelle}} = \frac{\mathrm{pH}^{\mathrm{bulk}} + \log_{10}(C_{\mathrm{salt}})}{2} + \frac{pK_a - \log_{10}(\rho_0^{\mathrm{micelle}})}{2}. \quad \textbf{[S50]}$$

Therefore, the prediction is that the local pH within the aggregates will increase linearly, with a slope of ½, with bulk pH and $\log_{10}(C_{\mathrm{salt}})$ (as observed in Fig. 4*D*), providing that $\log(\rho_0^{\mathrm{micelle}})$ does not vary too much with solution conditions. This simple model does not make predictions about this point, but an inspection of the predictions of the molecular theory confirms the approximated validity of such assumption. For instance, the volume fraction inside the micelles stays within the range 0.45–0.65 for all the conditions in Fig. 4*D* and, thus, $0.83 < \log(\rho_0^{\mathrm{micelle}}/\mathrm{M}) < 1.0$.

Not-regulating polyelectrolyte.
In this case, the concentration of segments inside the aggregates, $\rho_{\mathrm{Qpol}}^{\mathrm{micelle}}$, is fixed and independent of bulk pH and ionic strength (i.e., Eq. **47** is no longer valid). We can rearrange Eq. **45** as

$$\mathrm{pH}^{\mathrm{micelle}} = \mathrm{pH}^{\mathrm{bulk}} + \log_{10}(C_{\mathrm{salt}}) - \log_{10}(\rho_{\mathrm{Qpol}}^{\mathrm{micelle}}) \quad \textbf{[S51]}$$

and, thus, the pH inside the aggregates scales linearly with bulk pH and $\log_{10}(C_{\mathrm{salt}})$ with a slope of one. This is in good agreement with the slope predicted by solving the 3D molecular theory keeping fixed the value of f_c (Fig. S3).

1. Szleifer, I, Carignano, MA (1996) Tethered Polymer Layers. *Adv Chem Phys* 96:165–260.
2. Gong, P, Genzer, J, Szleifer, I (2007) Phase behavior and charge regulation of weak polyelectrolyte grafted layers. *Phys Rev Lett* 98:018302–018304.
3. Nap, R., Gong, P. & Szleifer, I., Weak polyelectrolytes tethered to surfaces: Effect of geometry, acid-nase equilibrium and electrical permittivity. *Journal of Polymer Science: Part B.* **44**, 2638–2662 (2006).
4. Tagliazucchi, M., Calvo, E.J. & Szleifer, I., Molecular theory of chemically modified electrodes by redox polyelectrolytes under equilibrium conditions: Comparison with experiment. *J Polym Sci Part B* **112**, 458–471 (2008).
5. Carignano, M.A. & Szleifer, I., Statistical thermodynamic theory of grafted polymeric layers. *J Chem Phys* **98**, 5006–5018 (1992).
6. Flory, P.J., *Statistical Mechanics Of Chain Molecules.* (Interscience Publishers, New York, 1969).
7. Gong, P, Wu, T, Genzer, J, Szleifer, I (2007) Behavior of surface-anchored poly(acrylic acid) brushes with grafting density gradients on solid substrates: 2. Theory. *Macromolecules* 40:8765–8773.
8. Ohshima, H. & Ohki, S., Donnan potential and surface potential of a charged membrane. *Biophys J* **47**, 673–678 (1985)

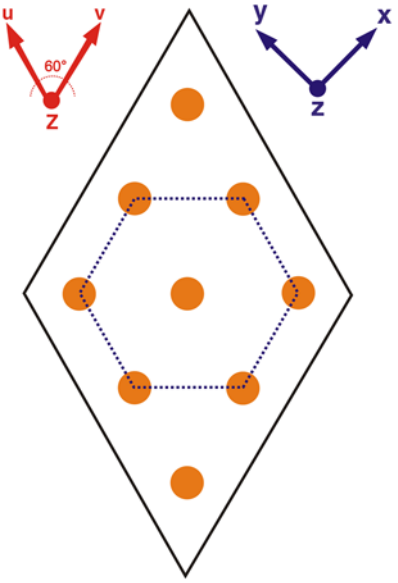

Fig. S1. Periodic cell used in the work with the grafting sites arranged in a hexagonal pattern (*Orange Circles*). The cell used in the work contained 64 different chains instead of 9.

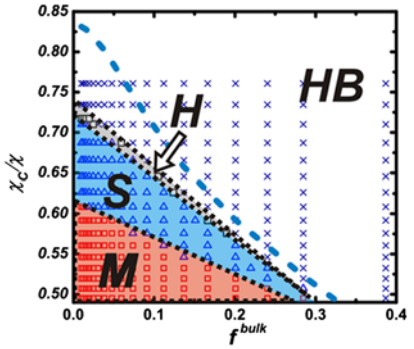

Fig. S2. Morphology diagram for a not-regulating polyacid layer. The plane shown corresponds to bulk dissociation fraction (f^{bulk}) as a function of the effective hydrophobicity of the backbone (χ_c/χ). This figure corresponds to the lower diagram in the Fig. 1 with the difference being that the diagram is plotted here as a linear function of f^{bulk}. Each symbol is obtained by solving the 3D theory for a given set of experimentally controlled variables. Different symbols and uppercase letters indicate the resulting morphologies: *M* (*Squares*), micelles; *S* (*Triangles*), stripes; *H* (*Circles*), holes; and *HB* (*Crosses*), homogeneous brush. $N_P/A = 0.111$ chains/nm^2, n (segments per chain) $= 50$, $l = 0.35$ nm (polymer segment length), $C_{salt} = 0.1$ M, and pK$_a = 5.0$ were used in the calculations.

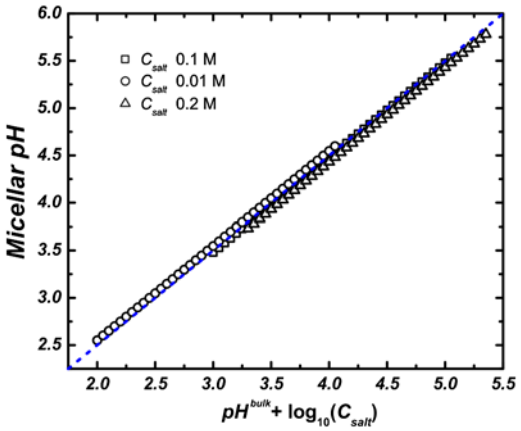

Fig. S3. Local pH inside quenched (not regulating) polyelectrolyte micellar aggregates for fixed fraction of charged segments ($f_c = 0.05$) as function of the relevant positive ions bulk concentrations. The *Dashed Blue Line* has a slope of one, as predicted by Eq **51**. Calculations correspond to: $\chi_c/\chi = 0.53$, $n = 50$, $N_P/A = 0.111$ chains/nm^2, and pKa $= 5.0$.

Table S1. Molecular details of the species in the system.

	Electrostatic charge, q_i	Molecular (segment) volume, v_i
Water	0	30 Å^3
Salt Cation	+1	33.5 Å^3
Salt Anion	−1	33.5 Å^3
Proton	+1	30 Å^3
Hydroxyl ions	−1	30 Å^3
Polymer Segment	−1 (pK$_a = 5.0$)	110 Å^3